Received: 1 December 2021 | Revised: 21 June 2022 | Accepted: 30 June 2022

DOI: 10.1002/hyp.14649

RESEARCH ARTICLE

WILEY

Large-scale lateral saturated soil hydraulic conductivity as a metric for the connectivity of subsurface flow paths at hillslope scale

Mario Pirastru[1] | Massimo Iovino[2] | Roberto Marrosu[1] | Simone Di Prima[1] | Filippo Giadrossich[1] | Hassan Awada[1]

[1]Department of Agricultural Sciences, University of Sassari, Sassari, Italy

[2]Department of Agricultural, Food and Forest Sciences, University of Palermo, Palermo, Italy

Correspondence
Mario Pirastru, Department of Agricultural Sciences, University of Sassari, Viale Italia 39a, 07100, Sassari, Italy.
Email: mpirastru@uniss.it

Funding information
Regione Autonoma della Sardegna; Università degli Studi di Sassari

Abstract

Lateral saturated soil hydraulic conductivity, $K_{s,l}$, is the soil property governing subsurface water transfer in hillslopes, and the key parameter in many numerical models simulating hydrological processes at the hillslope and catchment scales. Likewise, the hydrological connectivity of the lateral flow paths plays a significant role in determining the rate of the subsurface flow at various spatial scales. This study investigates the relationship between $K_{s,l}$ and hydrological connectivity at the hillslope spatial scale. $K_{s,l}$ was determined by the subsurface flow rates intercepted by drains and water table depths observed in a well network. The hydrological connectivity was evaluated by the synchronicity among water table peaks, and between these and the peaks of the drained flow. Rainfall and soil moisture were used to investigate the influence of the transient hydrological soil condition on connectivity and $K_{s,l}$. As the synchronicity of the water table response between wells increased, the lag times between the peaks of water levels and those of the drained subsurface flow decreased. Moreover, the most synchronic water table rises determined the highest drainage rates. The relationships between $K_{s,l}$ and water table depths were highly non-linear, with a sharp increase in the values for water table levels close to the soil surface. Estimated $K_{s,l}$ values for the full saturated soil were in the order of thousands of mm h^{-1}, suggesting the activation of macropores in the root zone. The $K_{s,l}$ values determined at the peak of the drainage events were correlated with the indicators of synchronicity. The sum of cumulative rainfall and antecedent soil moisture was correlated with the connectivity indicators and $K_{s,l}$. We suggest that, for simulating realistic processes at the hillslope scale, the hydrological connectivity could be implicitly considered in hydrological modelling through an evaluation of $K_{s,l}$ at the same spatial scale.

KEYWORDS
anisotropy, drain, hydraulic conductivity, hydrological connectivity, macropores, synchronicity

1 | INTRODUCTION

In humid climates and semiarid regions, hillslopes govern the hydrological response and transport nutrients and solutes in catchments (Anderson et al., 2009; Bachmair & Weiler, 2014; Haught & Meerveld, 2011; van Schaik et al., 2008). Lateral subsurface flow is one of the most critical processes in generating runoff in hillslopes (McDaniel et al., 2008; Weiler et al., 2006). Lateral preferential flow occurring under gravity, either in macropores or pipes, often dominates subsurface flow in natural hillslope (Scherrer et al., 2007; Sidle et al., 2000; Uchida et al., 2001). Understanding the processes and mechanisms that affect hydrological dynamics in the hillslope steep soil is essential for appropriate conceptualization and parameterization of numerical simulation models. These have been used to evaluate land use or climate change scenarios or test hydrological behaviour hypotheses (Kim & Mohanty, 2016; Niedda et al., 2014). In the last decades, several efforts of the hydrological community have been devolved into the experimental investigation of dynamics in hillslopes. These include hydrological measurements, use of tracers, modelling, or the integration of some or all these techniques (Anderson et al., 2009; Bachmair & Weiler, 2014; Haught & Meerveld, 2011; Hopp & McDonnell, 2009; Ocampo et al., 2006; Pirastru, Bagarello, et al., 2017; Pirastru, Marrosu, et al., 2017).

The lateral saturated hydraulic conductivity, $K_{s,l}$, is the soil property that primarily influences lateral water transport in hillslopes, and it is the crucial parameter in many numerical models simulating hydrological processes both at the hillslope and catchment scales (Matonse & Kroll, 2013; Niedda & Pirastru, 2014; Troch et al., 2003). Several low-cost and straightforward methods can estimate the hydraulic conductivity at the point scale (e.g., constant or falling head methods or borehole permeameter). However, there is a consensus that such evalutation is not sufficient to represent the effect of spatial heterogeneity (e.g., macropores) on the hydrological response at a larger spatial scale, for example, at the hillslope scale (Brooks et al., 2004). Probably, the most suitable approach for retrieving large scale $K_{s,l}$ values and studying the mechanism involved in the subsurface flow generation is excavating open trenches or installing drains to intercept the saturated subsurface flow moving above an impeding layer (Anderson et al., 2009; Bachmair et al., 2012; Brooks et al., 2004). For providing $K_{s,l}$, these measurements are generally associated with observation of the perched water table levels upslope of the trenches or drains so that Darcy's law could be applied together with outflow measurements. Measurements on trenches or drains represent an efficient way for retrieving soil hydraulic properties averaging local heterogeneities in the hillslope, including the spatially and temporally variable macropore network. However, such measurements are labor-intensive and expensive, and so far, only a few investigations have been reported in the scientific literature. Brooks et al. (2004) determined the hillslope-scale $K_{s,l}$ by drainage measurements performed on an 18-m wide isolated sloped land. The $K_{s,l}$ increased abruptly near the surface due to flow activation in the near-surface macropores of biological origin. The observed hillslope-scale $K_{s,l}$ was 3.2–13.7 times greater than the point-scale measurements. Brooks et al. (2007) achieved a good model agreement with observed perched water table readings and surface runoff in a grid-based model using the $K_{s,l}$ relationship determined at the hillslope scale by Brooks et al. (2004). Montgomery and Dietrich (1995) reported large-scale $K_{s,l}$ determined by the discharge of a gully cut with evidence of macropore flow. The $K_{s,l}$ was comparable with the greatest point-scale conductivity obtained by falling-head tests in piezometers. Chappell and Lancaster (2007) applied several field methods (i.e., slug test, constant- and falling-head borehole permeameter, ring permeameter, and two types of trench tests) to determine $K_{s,l}$. The $K_{s,l}$ determined by the trench percolation tests were, on average, 37 times larger than the mean conductivity obtained at the point spatial scale. Moreover, the same findings were confirmed by hydrological models calibrated with the catchment's observed hydrologic response (Blain & Milly, 1991; Chappell et al., 1998; Niedda, 2004). These models yielded $K_{s,l}$ values several orders of magnitude greater than those available at the point-scale. The discrepancies between point-scale and large-scale $K_{s,l}$ were generally attributed by the modellers to the large-scale effects of macropore flow, which local $K_{s,l}$ measurements do not capture. The difficulty in determining a representative $K_{s,l}$ value at a large spatial scale reduced the attempts to determine experimentally this soil property and pushed towards representing it as a calibrated parameter in modelling approaches. However, Sherlock et al. (2000) indicated that the differences between the measured and calibrated hydraulic conductivities could be attributed to the conceptual simplifications of the hydrological model structure and errors in estimating the other parameters involved. Hence, to represent realistic internal hydrological processes in models, independent estimates of $K_{s,l}$ at the operational simulation scale (pixel with areas of tens or hundreds of square meters) should be recommended. In this context, efforts by hydrologists should be directed to experimentally determine the value of this property at the spatial scale of interest.

Hydrological connectivity of lateral flow plays a significant role in many surface and subsurface landscape processes at various temporal and spatial scales (Bachmair & Weiler, 2014; Hopp & McDonnell, 2009; Sidle et al., 2001; Smith et al., 2010). Several studies indicated that hydrological connectivity directly affects water, chemistry, sediment, and biological processes in the hydrological systems. Meanings of connectivity differ depending on the specific application or context (see Michaelides & Chappell, 2009, for a review). From a hydrological point of view, connectivity implies an exchange of mass and energy between spatially well-defined discrete units of a system (for example, hillslope-floodplain-river channel as in Ocampo et al., 2006, or in Penna et al., 2015). However, the bounds of hydrological compartments are not always identified over the space, so connectivity could also be defined as "…the condition by which disparate regions on the hillslope are linked via subsurface flow…" (Stieglitz et al., 2003). In this framework, Bachmair and Weiler (2014) argued that a combination of observations at different spatial scales and the consideration of the high spatial variability of subsurface spatial flow at plot and hillslope spatial scale are needed for assessing hydrological connectivity. Tromp-van Meerveld and McDonnell (2006) suggested that evaluating the spatial pattern of subsurface flow pathways and

connectivity was the key to conceptualizing the non-linear process of subsurface stormflow. Anderson et al. (2009) showed that the connectivity of the hillslope preferential flow network governed the subsurface flow velocity in hillslopes.

Studies on connectivity try to find symptoms by observing variables of state (water table, soil moisture) or geochemistry dynamics. Generally, threshold behaviour or synchronic reaction of local responses (e.g., water table responses to precipitation) manifests spatial connectivity (Bachmair & Weiler, 2014; Haught & Meerveld, 2011; Penna et al., 2015). Contrarily, when units of the system (e.g., upland and riparian zones) behave independently and differently, those parts are seen as disconnected from each other. Dynamic connectivity provides a qualitative description of a transient hydrological state, which needs to be performed with reference to a large spatial scale (tens or hundreds of square meters). However, a numerical indicator of connectivity is not easy to find. The need to evaluate the connectivity in a hydrological system is apparent in modelling studies. Hydrological and biogeochemistry simulations are not accurate or realistic without understanding the evolution of connected flow paths within the subsurface and on the surface of hillslopes and catchments (Kim & Mohanty, 2016; Wienhöfer & Zehe, 2014). The need for an appropriate representation of the connectivity in hydrological modelling appears more evident in grid-based distributed hydrological models. Here, the minimum scale of modelling of the processes depends on a series of factors, including computational burden, spatial heterogeneity (e.g., soil use and surface morphology) and availability of hydrological data for calibrating and validating the models. In addition, the choice of the modelling grid-size should depend on our knowledge of the spatial heterogeneity in soil hydraulic properties and soil thicknesses. Freer et al. (2002) showed the importance of detailed knowledge of soil thicknesses for correctly representing the connectivity of the subsurface flow paths in a hillslope. The virtual experiments of Hopp and McDonnell (2009) suggested that misrepresenting some soil variables (soil depth, slope angles, bedrock permeability) can result in very different simulations of the connected flow paths. As concluded by Brooks et al. (2007), "the accuracy of any distributed hydrological model is limited by our ability to characterize the heterogeneity." Nowadays, hydrologists still have limited tools for studying spatial heterogeneity of the soil properties (particularly hydraulic conductivity and connectivity) or the soil thicknesses over large areas. Consequently, in distributed hydrological modelling, coarse grid sizes (from tens to hundreds of m^2) are frequent. Increasing the size of the spatial modelling unit also increases the need to adequately represent the hydrological effects of the large-scale hydrological connectivity of the flow paths in the soil. This is particularly evident in basins or hillslopes with natural vegetation and undisturbed soils, where the connectivity of the macropore network governs the subsurface flow rates (van Schaik et al., 2008). As also suggested by the study of Pachepsky and Hill (2017), macropore flow cannot be seen at the small scale but emerges and becomes of interest at the plot or larger spatial scale. To account for these effects, Niedda (2004) developed a scaling relation that linked the soil hydraulic conductivity evaluated at the point-scale with that much higher required at the typically coarser modelling scales. In the case of large spatial model units, the appropriate parameterization of soil hydraulic properties remains one of the greatest challenges. In particular, hydrological connectivity is rarely included in model parameterization due to the difficulty of providing a measurable connectivity parameter.

When the regions of a hydrological system are connected, the system's efficiency in conducting water between internal regions and towards the outside is greatly improved. Peaks of streamflow or chemistry release have been observed when transient hydrological conditions favour spatial connectivity of lateral subsurface flow (high soil moisture, perched water table formation)(Anderson et al., 2009; Buttle & McDonald, 2002; Ocampo et al., 2006). The lateral saturated hydraulic conductivity of a system evaluates the ability to transfer water downslope (under defined hydraulic gradient). Hence, $K_{s,l}$ determined at the same spatial scale where the spatial connectivity mostly affects hydrological dynamic (e.g., hillslope scale) should embed information on connectivity. This is the general idea behind this research work, where hydraulic conductivity is estimated at the hillslope scale, and linkages with indicators of hydrological connectivity are searched.

The general objective of the research is to investigate the relationship between lateral saturated hydraulic conductivity and hydrological connectivity at the hillslope spatial scale. The investigation was performed in a steep hillslope of the Baratz catchment in Sardinia (Niedda et al., 2014; Niedda & Pirastru, 2013). The hillslope response was investigated with reference to subsurface flow intercepted by drains with different dimensions. The first dataset was collected for 2014–2015 by a 2.5 m long drain, called a short drain; then the drain was lengthened to 8.5 m (hereafter called a long drain), and a second dataset was collected in 2016–2017. Pirastru, Bagarello, et al. (2017) reported the details on the methodology of the investigation and the results of the short drain. In this paper, their findings are recalled for comparison with the results of the long drain investigation. The differences observed in the relationships between the lateral saturated hydraulic conductivity and the water table depth for the short and long drains will be evaluated in terms of hydrological connectivity of the soil macropore network.

In summary, the specific objectives of the study are:

i. Establishing the role of the dynamic hydrological connectivity of the lateral subsurface flow paths in governing the hydrological response in the studied hillslope;
ii. Evaluating if the lateral saturated hydraulic conductivity estimated at the hillslope scale could be an indicator of dynamic hydrological connectivity at the same spatial scale;
iii. Evaluating if the spatial variability of hydrological connectivity could explain the observed differences in the drainage behaviour and in the $K_{s,l}$ relationships obtained for the short and long drains.

2 | MATERIAL AND METHODS

2.1 | Site description

The area is a steep side slope (Figure 1a) located in the Baratz Lake catchment, northwestern coast of Sardinia, Italy (40.6982' N, 8.2346' E; WGS84). The climate is the semiarid Mediterranean, usually

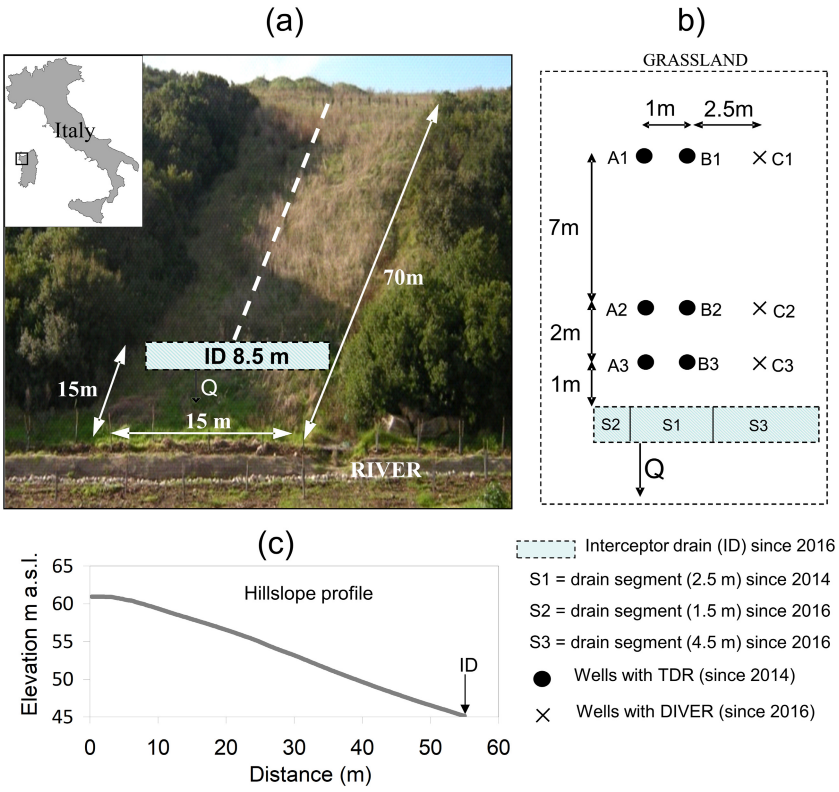

FIGURE 1 (a) View of the experimental hillslope, with the location of the interceptor drain (ID); (b) positioning of well network with respect to the drain. The drain segments realized in 2014 (S1) and 2016 (S2 and S3) are shown; (c) elevations of the hillslope measured along a central line (dashed line in 1a). The setup is not drawn to scale

featuring mild winters, warm summers, and a high water deficit from April to September. Mean annual temperature and relative humidity are about 16°C and 78%, respectively. The average annual precipitation is about 600 mm, mainly falling from autumn to spring. The potential evapotranspiration is around 1000 mm per year.

The experimental hillslope ranges from 51 to 65 m a.s.l.; it is about 60 m long, with 30% slopes (Figure 1c). The surface morphology is predominantly planar, slightly concave in the upper part of the hillslope. The incoming surface and subsurface flows in this upper part are diverted by ditches existing on both sides of the road and thus are excluded from the experimental hillslope. At the toe, the hillslope is drained by the main stream channel of the catchment. The soil is Lithic Haploxerepts, with a depth ranging from 0.3 to 0.5 m. Soil horizons are Ap (0–0.15 m), approximately deep as the root zone, BW (0.15–0.50 m), and C. The C horizon is a dense altered Permian sandstone acting as impeding layer (K_s <1 mm h^{-1}). The experimental area is covered mainly with spontaneous grass grown after the clearing of the Mediterranean maquis and a deep moldboard ploughing about 15 years ago, likely to create a 15-m wide firebreak. The grass is cut only one time per year.

2.2 | Subsurface flow, groundwater, and rainfall monitoring

The experimental scheme was set up in January 2014 to monitor the lateral saturated subsurface flow, groundwater levels, and soil moisture above the impeding layer. For this scope, a 2.5 m interceptor drain (S1 drain segment in Figure 1b) was installed centrally in the grassed area (Pirastru, Bagarello, et al., 2017). A trench was hand dug until the impeding layer was reached. The downslope wall and the bottom of the trench were sealed with concrete. A perforated drainage line wrapped with geotextile was placed on the bottom of the trench to collect the drained water and deliver it to the measuring system. Finally, the trench was filled with fine gravel to maximize the conductivity of the drain. The outflow was routed in a plastic box with a 60° V-notch weir outlet. The water head over the V-notch was measured by a stand-alone pressure transducer every 5 min and associated with the flow rate by the weir formula. The outgoing flow from the box dropped into an automated tipping bucket (about 2×10^{-3} L/tip), thus providing a more accurate measure of the flow rate when it was smaller than 0.4 L min^{-1}. Six shallow monitoring wells were drilled at 1, 3, and 10 m upslope of the drain (wells from A1 to B3 in Figure 1b). The depth of the wells varied from 0.35 to 0.45 m, with the last centimetres included in the impeding layer. The wells were equipped with automated WCR probes (Campbell Scientific Inc. CS616 Water Content Reflectometer) standing vertically in the wells to measure the water levels. A fifth polynomial relationship between the WCR output and the percentage of rod submergence was calibrated in the laboratory. This value is corrected with the reference depth of the probe in the field to determine the water table depths. As the probe rods were shorter than the soil thickness, they were periodically moved up or down in the wells to remain partially submerged. The obtained water table levels were validated by manual measurements collected throughout the monitoring periods to evaluate the accuracy with high and low water table levels. The mean

absolute error between the values of water levels estimated by the calibrated WCR output and those measured manually in the field was less than 0.01 m. This error was considered negligible for the investigation. Soil moistures were monitored by three CS616 probes placed at three elevations in the hillslope close to the A and B well alignments. The probes were installed vertically in the soil to estimate the mean soil moisture in the first 0.3 m.

In January 2016, the monitoring scheme was spatially increased. The 2.5 long drain was prolonged by two new segments (S2 and S3 in Figure 1b) to realize an 8.5 m long drain. The procedures for realizing the additional segments were the same described for the short drain. An automated 0.5 L tipping bucket flowmeter (maximum working flow rate of 25 L min^{-1}) measured the outflow from the drain. Three new wells were drilled to form a third well alignment (wells from C1 to C3). A Schlumberger mini-Diver recorded the water table height in each of these new wells with its own storage memory.

An automatic weather station recorded rainfall near the studied hillslope from January 2014 to December 2016 and from March to July 2017. Periods of lacking rainfall data were filled with data from the closest available weather stations, Olmedo and Capocaccia stations, both approximately 10 km far from the experimental area. All the hydrological measurements were logged at a time step of 5 min.

2.3 | Estimation of the lateral hydraulic conductivities of the saturated soil

The lateral saturated soil hydraulic conductivities, $K_{s,l}$ [LT^{-1}], were computed by Darcy's law:

$$K_{s,l} = -q \cdot D^{-1} \cdot \frac{ds}{dZ}, \quad (1)$$

where q [L^2 T^{-1}] is water flow drained per width unit of the drain, D [L] is saturated soil thickness above the impeding layer determined in the cross-sectional flow area, Z [L] is water table elevation above an arbitrary datum, s is the distance measured along the flow direction [L]. dZ/ds is the total gradient term, negative along the flow direction. Dupuit–Forchheimer approximation for the case of drainage of an unconfined aquifer resting on the sloping bed (Childs, 1971) was the basic assumption to apply Darcy's law.

The transient water levels in the well network were used to evaluate the saturated soil thicknesses and the total gradient terms in Equation (1). To obtain D, the mean water table depths at the three elevations i in the hillslope (WTDi, with $i = 1, 2, 3$, see Figure 1b) were calculated. Thereafter, the correlations between q and WTDi were checked, and the WTDi with the highest correlation with q was used along with the soil thickness to determine the D values. dZ/ds values were determined as the average of the gradient terms closest to the drain (computed between A2–A3, B2–B3, and C2–C3) to have the best estimate of the gradients that effectively drove the drain response.

2.4 | Hydrological analysis for the drain data

Storms with precipitation greater than 3 mm were classified as events. Rain events were considered distinct when at least 6 h passed from the last rain pulse of the considered event and the first rain pulse of the successive event.

Event runoff coefficients were computed as the ratio between drainage (mm) and total rainfall (mm). The drainage volume (m^3) attributed to a rain event was computed from the first drainage pulse observed in response to rainfall until the end of the drainage. For two partially superimposed drainage events, the drainage tail of the first event was simulated by a power-law decay function precisely calibrated for that event, and the simulated volume was subtracted to the successive event. The conversion from m^3 to mm of drainage considers the contributing areas, estimated by multiplying the drain length (2.5 or 8.5 m) by 55 m (i.e., the distance from the drain to the upper end of the hill, Figure 1c).

The correlation analyses between the hydrological data were performed by the non-parametric Spearman rank method (Haught & Meerveld, 2011). This approach was chosen due to the general non-linearity of the found relationships. The Spearman coefficient, ρ, and the p-value for the statistical significance were computed for each tested relationship. Unless differently stated, a p-value of 0.001 defined the considered threshold for the statistical significance. For consistency of the analyses, only periods with all the instruments functioning were considered.

The timing of the water table responses, the antecedent soil moisture (ASM), and the rainfall (P) were analysed to evaluate the role of the connectivity on the hydrological response of the hillslope and on the computed hydraulic conductivities. In particular, for each drainage event and well, the lag time between the water table peak and the peak of maximum discharge rate were determined. Mean lag times (i.e., averaging all the wells), Δt_L, and standard deviations of lag times, SD, were evaluated for the 35 most relevant drainage events in the monitoring period from 2016 to 2017. Events from 2014 to 2015 were not considered for this analysis because of the difficulty in precisely determining the instant of drainage peaks due to the water level oscillations in the discharge measurement device.

Antecedent soil moisture (ASM), rainfall (P), and ASM + P were determined in a subset of 17 drainage events mainly occurring from January to April 2016, when we had detailed precipitation data measured close to the experimental area. ASM was determined at the start of the rainfall by multiplying the averaged volumetric soil water content (m^3 m^{-3}) estimated by the three WCR probes and the soil depth explored by rods (30 cm). P, ASM, and ASM + P are expressed as water depth (mm).

3 | RESULTS

3.1 | Discharge data and runoff coefficients

About one hundred rainfall events occurred during the monitoring years from 2014 to 2017, and 75% of these events caused drainage

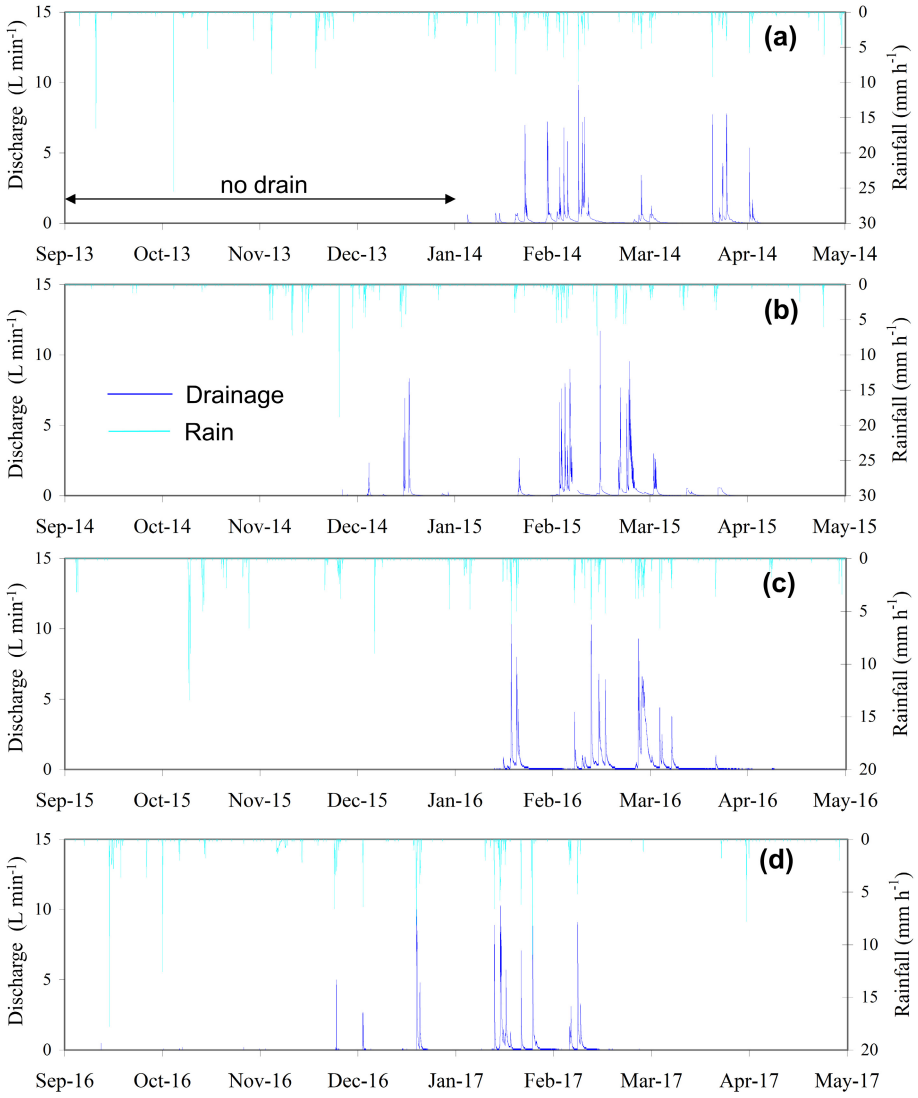

FIGURE 2 Time series of observed precipitation and drainage from the hillslope: (a and b) outflow from the 2.5-m long drain; (c and d) outflow from the 8.5-m long drain

	2014[a]	2015[a]	2016[b]	2017[b]
N° events	20	24	18	15
Mean rainfall depth (mm)	11.68 (0.56)	12.67 (0.54)	11.39 (0.72)	16.06 (0.58)
Mean runoff coefficient (–)	0.88 (0.48)	0.87 (0.65)	0.41 (0.63)	0.23 (0.96)
Max drainage volume (m^3)	3.59	2.76	12.57	5.87
Mean drainage volume (m^3)	1.32 (0.70)	1.49 (1.04)	2.60 (1.18)	1.72 (1.04)
Max discharge (L min^{-1})	9.80	11.70	12.24	11.00
Mean of peak discharges (L min^{-1})	4.87 (3.52)	5.06 (3.02)	4.91 (3.61)	5.10 (2.88)

TABLE 1 Statistics of precipitation and drainage events from 2014 to 2017

Note: Statistics consider only events with outflow greater than zero. Standard deviation is between parentheses.
[a]drain 2.5 m long.
[b]drain 8.5 m long.

responses (Figure 2). We consider a hydrological year starting from September. Basic statistics of the generated 5-min drainage peaks and the drained volumes are reported in Table 1 for each hydrological year. Compared to the 2014–2015 period, the mean and maximum values of the peak rates of the drainage events did not change significantly after January 2016. Conversely, the mean and maximum drainage volumes per event did show considerable changes but the increases were not proportional to the drain lengthening. Figure 3 depicts the computed event runoff coefficients. With the 2.5 m long drain, approximately half of the runoff coefficients were higher than

one, and in two occasions even higher than two. In the years 2016 and 2017, the runoff coefficients were generally lower than one, and close to one only in a case.

3.2 | Water table depths, subsurface flow rates and estimated $K_{s,l}$ values

Figure 4 shows a boxplot of the observed water table depths in the monitoring period 2016–17. A sole plot for the two monitoring years is proposed because the statistics were similar between the 2 years. Moreover, the statistics of the wells from A1 to B3 were similar to those shown in Pirastru, Bagarello, et al. (2017) for the 2014–15 years, indicating that extending the drain line did not alter significantly the drainage dynamic in the portion of the hillslope upslope the S1 drain segment. From Figure 4, it can be seen that the water table thickness along the same elevation contour is not uniform. Regarding the wells closest to the drain, used for the flow cross-sectional area estimation (through the D value in Equation (1)) and for the gradients as described later, the water table thickness in average (i.e., mean water table depth minus the depth of the impeding layer) is 0.27 m in the well C3, and close to 0.15 m in both the wells A3 and B3. Moreover, C3 showed greater variability than the other wells. Clearly, by monitoring only three points along a contour, we can characterize only partially the spatial variability of the water table thicknesses. This introduces uncertainty in determining the effective cross-sectional flow area and the hydraulic gradients in the $K_{s,l}$ calculation.

The water level fluctuations measured in the wells located at the same elevation in the hillslope were consistently correlated. The maximum and minimum ρ, both found in the 2017 monitoring year, were 0.97 and 0.82, respectively (Table 2). These values were detected with reference to the well pairs A3–B3 and B1–C1. Similar correlations were also observed during the 2014 and 2015 years (Pirastru, Bagarello, et al., 2017). Considering the consistency between observations in the wells, averaged water levels were computed between wells located at the higher, intermediate, and lower elevations in the hillslope and named WTD_1, WTD_2, and WTD_3, respectively.

Figure 5 depicts WTD_1, WTD_2, and WTD_3 against q for each hydrological year from 2014 to 2017 and the computed ρ coefficients. Correlation coefficients lower than −0.82 indicated a close relationship between the water table dynamic and the drained subsurface flow. The correlation coefficients were similar for the 2016 and 2017 years (long drain) and the 2014 and 2015 periods (short drain), thus showing temporal stability in the q versus WTD relationships. The observed significant correlations also indicated that the groundwater response in the monitored area, which was only a portion of the hillslope, was in line with the drain response, which instead integrated the hydrological response of the whole hillslope.

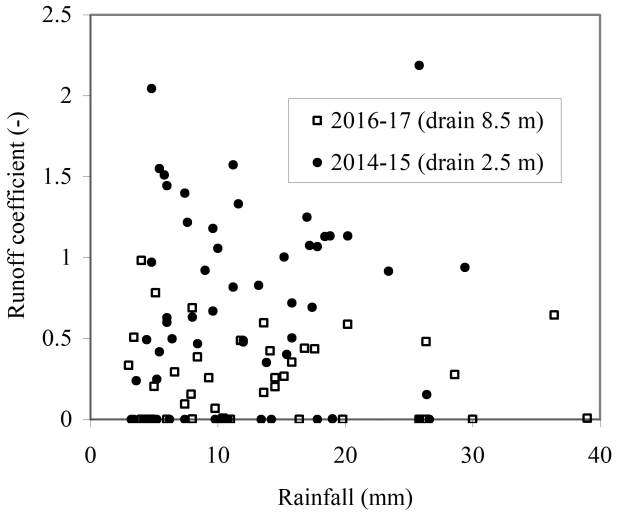

FIGURE 3 Runoff coefficients for the rainfall events from 2014 to 2017

TABLE 2 Spearman correlation coefficients, ρ, computed in 2016 and 2017 between wells located at the same elevation in the hillslope

A-B alignments	A-C alignments	B-C alignments
A1-B1*	A1-C1*	B1-C1*
0.91 (0.91)	0.86 (0.84)	0.92 (0.82)
A2-B2*	A2-C2*	B2-C2*
0.94 (0.91)	0.9 (0.93)	0.92 (0.85)
A3-B3*	A3-C3*	B3-C3*
0.92 (0.97)	0.9 (0.91)	0.96 (0.88)

Note: The coefficients of 2017 are between parentheses.
*Statistically significant correlation at $p = 0.001$.

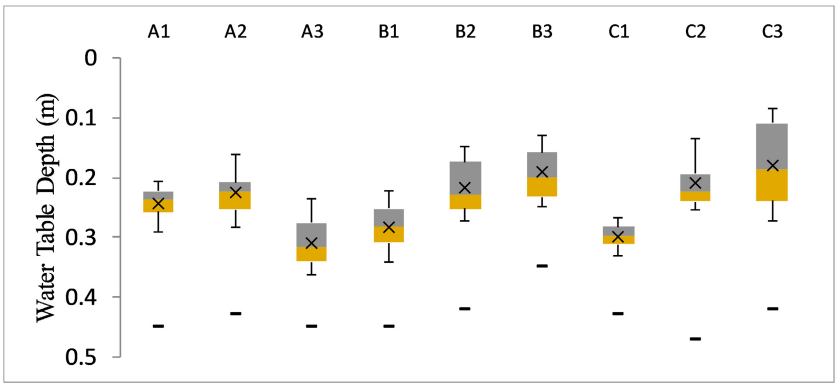

FIGURE 4 Boxplots of the water table depth in the monitoring wells from 2016–2017. The top and the bottom of the boxes determine the 25th and 75th percentiles, respectively. The lines through the boxes are medians; crosses within the boxes indicate means; the whiskers are the 10th and 90th percentiles. The black traits below the boxes indicate the depths of the impeding layer as documented during well drilling

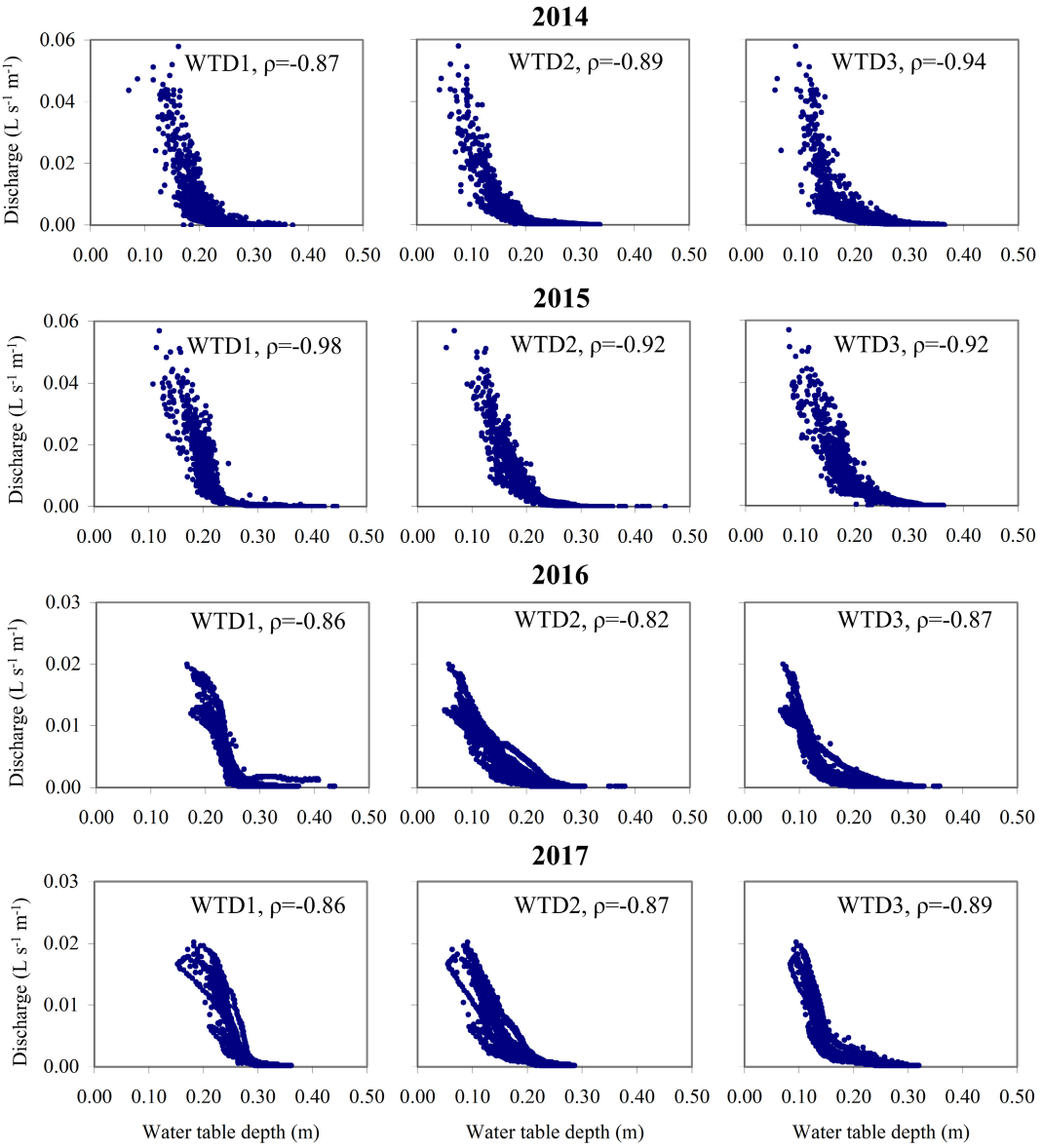

FIGURE 5 Relationships between observed mean water table depth at the higher, intermediate, and lower elevation in the hillslope (WTD1, WTD2, and WTD3, respectively) and drain discharge for monitoring years 2014–2015 (2.5-m drain, well alignment A–B), and 2016–2017 (8.5-m drain, well alignment A–B–C). ρ is the Spearman correlation coefficient

Generally, the water table depths in the wells closest to the drain, WTD_3, had the best correlations with the drainage rates (Figure 5). After that, we consider WTD_3 as a reference for the description of the relationships with the subsurface flow rate and the computation of the D values to be used in Equation (1). However, analyses conducted using WTD_1 or WTD_2 or an averaged water table depth computed considering all monitoring network wells gave similar results. Figure 6a shows the q versus WTD_3 relationship for the 2016–2017 years compared to the relationships obtained in the same period considering the wells A3, B3, and C3 one at a time. The averaged q versus WTD_3 appears similar to the ones obtained using water table depths from B3 and C3, while the A3 relationship, according to Figure 4, shifts towards greater values of water table depth. Owing to the similarity of the relationships between q and WTD_3 in 2014 and 2015 and 2016 and 2017, a q versus WTD_3 relationship was obtained for each 2-year period, representing a drain length. The two relationships, shown in Figure 6b, were highly non-linear. Subsurface discharges sharply increased for WTD_3 lower than about 0.15 m (i.e., the large thickness of the saturated layer), which was approximately the lower end of the Ap soil horizon. The q versus WTD_3 data ensemble is steeper for the short drain, and the maximum q values were about three times higher for the short drain than the long one.

Figure 7a and b show the $K_{s,l}$ values computed using the subsurface flow drained by the short (2.5 m) and long (8.5 m) drains, related to the observed discharges and WTD_3, respectively. There was a strong correlation between q and $K_{s,l}$ whatever drain length was considered. Power functions with exponents close to 0.8 well fitted the q versus $K_{s,l}$ relationships. Due to the high correlations between q and $K_{s,l}$

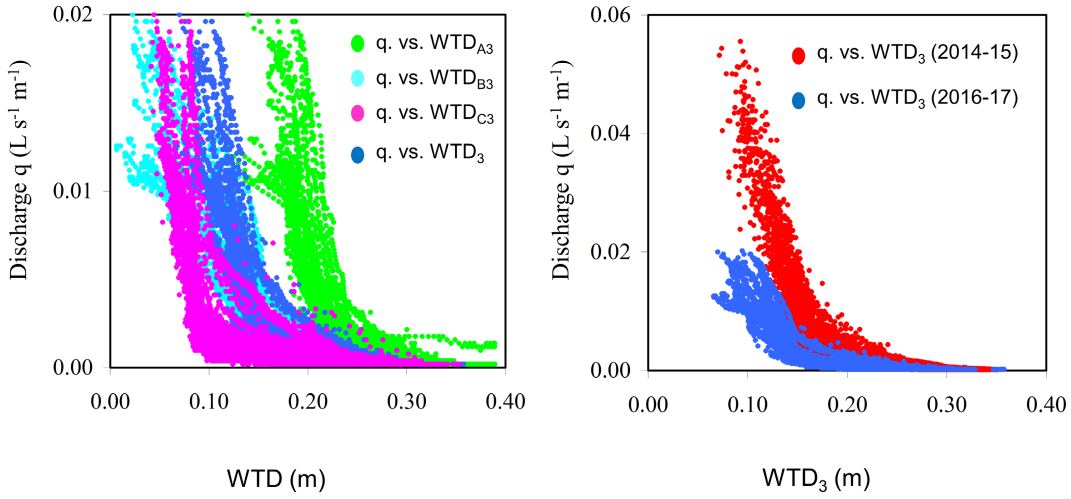

FIGURE 6 (a) Discharge per unit width of the drain, *q*, versus water table depths, WTD, observed in the wells A3, B3, and C3 in monitoring years 2016–2017 (long drain); q versus averaged water table depths, WTD_3, for the short (2014–2015) and long (2016–2017) drain

FIGURE 7 Lateral saturated hydraulic conductivity, $K_{s,l}$, estimated by the data of short (2.5 m) and long (8.5 m) drains, (a) versus drainage per unit with of drain, *q*, and (b) versus mean water table depth close to the drains, WTD_3

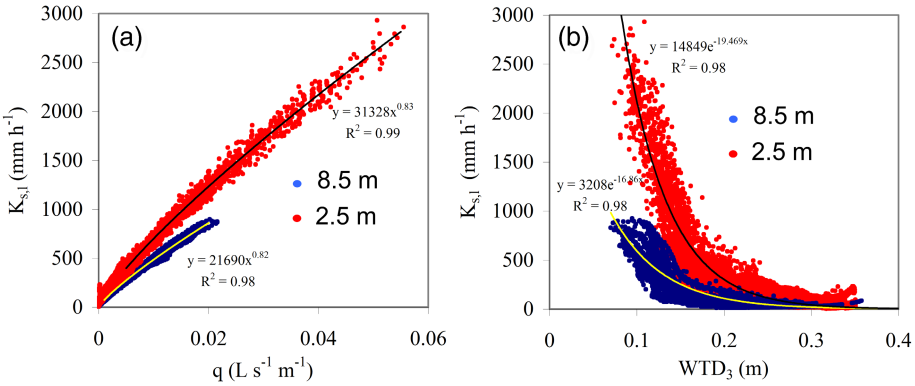

(Figure 7a), the estimated non-linear $K_{s,l}$ versus WTD_3 relationships (Figure 7b) closely resemble the observed *q* versus WTD_3 patterns.

3.3 | Relationships between water table timing, discharges, and $K_{s,l}$

Generally, the water table rise in the wells preceded the drain discharge peak (positive lag times). The lag times were, on average, shorter for the wells closest to the drain, and the wells located at the intermediate and high elevations in the hillslope responded on average at the same time. However, the temporal sequence of the activation of the wells changed from one event to another, indicating that other factors (e.g., local soil moisture) besides the positioning on the hillslope influenced the water table response. Moreover, we have to consider that the water table data acquisition interval was 5 min. In events with high rainfall intensity and high antecedent soil moisture, the lag time of the wells was in the order of 10 min or shorter. This introduced uncertainty in the exact determination of the lag time, which can be significant for the faster drainage events (short Δt_L). However, this uncertainty did not hinder capturing a general behaviour of the water table timing with respect to the drainage of the hillslope, as described below.

Figure 8a compares means, Δt_L, and standard deviations, SD, of the lag times computed between the peaks of groundwater observed in all the wells and the peaks of the subsurface flow drained from 2016 to 2017. The lower the Δt_L, the more synchronous the groundwater peaks with the peaks of the subsurface flow. The lower the SD, the more synchronous the water table peaks in the monitoring wells.

There was a statistically significant positive correlation between SD and Δt_L. In general, the more synchronous was the water table response between the monitoring wells, the shorter was the delay of the subsurface flow response compared to the water table response. This indicated increasing synchronicity between hydrological processes operating at different spatial scales. While the water table fluctuation at the discrete measurement points reflected processes that depend on local soil characteristics, for example, soil depth and local hydraulic conductivity, the drained subsurface flow integrated the spatial and temporal dynamics of the water table throughout the contributing hillslope.

Figure 8b shows a statistically significant inverse correlation of *q* with SD. Hence, the timing of the local water table change was

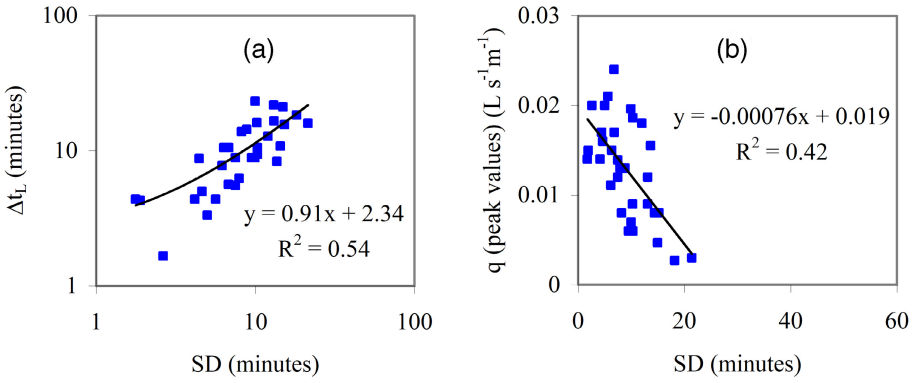

FIGURE 8 (a) Relationship between means (ΔtL) of the lag times (considering all the wells) and standard deviations (SD) for the drainage events in the years 2016 and 2017. The graph is plotted in log–log scale; (b) relationships between the *q* values determined at the drainage peaks and SD

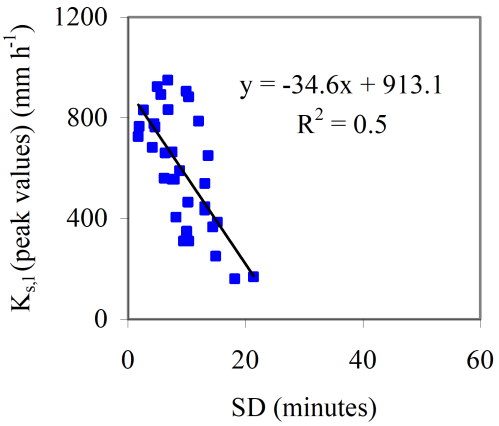

FIGURE 9 Relationships between the $K_{s,l}$ values determined at the drainage peaks and standard deviations (SD) of the lag times

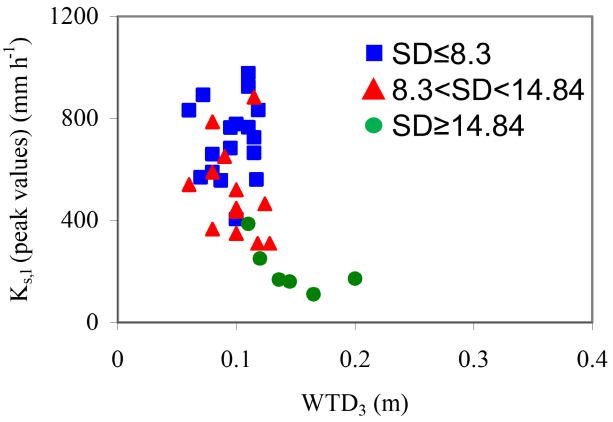

FIGURE 10 $K_{s,l}$ values vs. WTD_3, both determined at the drainage peaks, classified based on the standard deviation (SD) of the lag times

linked to the intensity of the hydrological response at the hillslope scale. A similar relationship could be realized between *q* and Δt_L. Significant correlations between *q* and mean lag times could also be yielded by considering the triplets of wells located at the high, intermediate, and low elevations in the hillslope (data not shown). The correlations appear clearer for the wells close to the drain (R^2 about 0.4 for both intermediate and low elevations) with respect to the farthest ones (R^2 = 0.27). Figure 9 shows the correlation of the lateral saturated hydraulic conductivity with SD. The observed high correlation is expected, considering the functional dependence between *q* and $K_{s,l}$ seen in Figure 7a. Figure 9 clearly illustrates that the $K_{s,l}$ determined at the hillslope scale depends on the synchronicity of hydrological processes that govern the groundwater dynamics in the hillslope (water fluctuations, subsurface flow transfer). Such synchronicity is considered a consequence of the hillslope's hydrological connectivity of the lateral flow paths. The dependency of $K_{s,l}$ on the synchronicity of the water table dynamic is further elucidated in Figure 10, which classifies the $K_{s,l}$ versus WTD_3 data pairs computed at the drainage peaks based on the SD values. Three classes of events were established following an equal-interval criterion. The characteristics of the three classes are reported in Table 3. All the classes differed statistically (Mann–Whitney unilateral test) for the $K_{s,l}$ values, confirming the importance of the synchronicity of water table rises, evaluated by SD, in determining the conductivity values. The WTD_3 values measured at the peaks of the drainage were not statistically different for the two classes with the lowest SD. Conversely, the WTD_3 values of the class with SD ≥14.84 significantly differed from the other classes. This indicated that the water table depth influenced the synchronicity of water table peaks for high WTD_3 (water table standing about in the lower half of the soil profile). However, it was independent of the water table depth when the groundwater was closer to the soil surface.

The control of the hydrological soil condition of the site on the timing of the water table responses and the hydraulic conductivity values was investigated by analysing the correlations of SD and $K_{s,l}$ with antecedent soil moisture condition (ASM), rainfall (P), and ASM + P, as proposed by Penna et al. (2015). The results are reported in Table 4.

$K_{s,l}$, and SD were significantly correlated with ASM + P, as shown in Figure 11a and b, respectively. Compared to ASM + P, rainfall depth showed a weaker correlation with SD and $K_{s,l}$. Finally, ASM was uncorrelated with all the considered variables (Table 4).

Examples of $K_{s,l}$ vs. WTD_3 relationships determined for selected drainage events with increasing ASM + P are reported in Figure 12. The greater the ASM + P index, the greater the $K_{s,l}$ value reached at the peak of the drainage event. The minimum reached WTD_3 values were close to 0.1 m for all the reported relationships; despite the

TABLE 3 Statistics of the classes of drainage events shown in Figure 9

Classes	SD≤8.3	8.3 < SD <14.84	SD ≥14.84
No. of events	15	13	6
mean $K_{s,I}$ (peak values) (mm h^{-1})	724.25 (153)	511.62 (178)	207.67 (98)
SD (minutes)	5.46 (2.07)	11.42 (1.85)	45.17 (43)
$\Delta t_L \Delta_{TL}$ (minutes)	6.58 (3.22)	13.76 (4.96)	37.61 (31.03)
WTD_3 (m)	0.097 (0.018)[a]	0.098 (0.019)[a]	0.146 (0.032)

Note: The first number is the mean; the standard deviation is in parentheses.
[a]Non-significant correlation with $K_{s,1}$.

TABLE 4 Spearman coefficients, ρ, of the relationships between antecedent soil moisture (ASM), precipitation (P), and ASM + P with the standard deviation of the lag times (SD) and $K_{s,I}$

Variable	SD	$K_{s,I}$
ASM	0.047 (0.86)	0.084 (0.75)
P	−0.46 (0.07)	0.63 (0.009)
ASM + P	−0.63 (0.009)	0.87 (<0.0001)

Note: In parentheses, the p-values for the statistical significance are reported.

maximum reached $K_{s,I}$ values ranged from 400 to 1000 mm h^{-1}. This was in line with Table 3, indicating differences in the mean $K_{s,I}$ values for the drainage events falling in the classes with SD ≤ 8.3 and 8.3 < SD <14.84, and no significant differences for the mean WTD_3 close to 0.1 m for both classes.

4 | DISCUSSION

4.1 | Spatial hydrological connectivity governs hillslope response

The water levels in the monitoring wells generally did not respond simultaneously to the rain input. When the water table responses tended to be more synchronous between the wells (low SD), their peak timing also matched that of the subsurface flow response (short Δt_L). In this situation, the hillslope provided the most intense hydrological responses (Figures 8b). Hence, the coupling between processes at the local (i.e., water table rise into the wells) and hillslope scale (i.e., drain discharge) was a primary mechanism governing the magnitude of the subsurface hydrological response in the studied system. The results of this study agree with other research (Haught & Meerveld, 2011; Penna et al., 2015) reporting that for the temporal series of streamflow events, the greater was the synchronicity of the water table responses in hillslopes, the lower were the mean lag times determined with respect to the streamflow peak, and the higher were the streamflow intensities. We propose that the observed variability in SD and Δt_L was caused by the temporal and spatial variability of hydrological connectivity of subsurface flow paths in the hillslope. This is in line with several studies (Anderson et al., 2009; Bachmair & Weiler, 2014; Hopp & McDonnell, 2009; Penna et al., 2015) reporting synchronicity between subsurface flow or streamflow and water table responses in hillslopes. The synchronicity among the water table peaks in the wells and between these and the drainage peaks changed depending on the transient soil hydrological condition in the hillslope. In particular, we found that SD decreased as the sum of the antecedent soil moisture and the rainfall depth increased (Figure 11b). Consequently, ASM + P could be used as a proxy variable to predict the hydrological connectivity at the hillslope scale. The results of the study agree with Penna et al. (2015) findings, showing the combined effect of storage and storm characteristics in governing the subsurface hydrological connectivity in the investigated basins. However, in our study, the connectivity was governed mainly by the rainfall depth, while ASM was a less determining factor given that it was uncorrelated with Δt_L and SD. This finding agrees with Anderson et al. (2009), and it was probably influenced by the generally high soil moisture content observed in the rainy periods where the drainage events occurred.

4.2 | $K_{s,I}$ as a metric of the hydrological connectivity at the hillslope scale

Figure 9, and Table 3, showed that the $K_{s,I}$ values determined at the drainage peaks were negatively correlated with SD (and with Δt_L, considering the existing high correlation between Δt_L and SD, Figure 8a). This suggested that the synchronicity of hydrological processes in the hillslope controlled the ability of the whole soil pore network to transmit the lateral subsurface flow downslope. Hence, the computed large-scale $K_{s,I}$ values embed information about the subsurface flow path connectivity controlling the hillslope's hydrological response.

It is widely recognized that macropores have a crucial role in determining the water transfer efficiency within heterogeneous hydrological systems, such as the hillslopes. A previous study performed on the same site by Di Prima et al. (2018) highlighted the effects of the macropores on the lateral anisotropy of the soil hydraulic conductivity. The K_s values (from 4 to 43 mm h^{-1}) yielded at the point-scale by a vertical infiltration method were consistently lower than the $K_{s,I}$ values determined by an in-situ large block method that included contribution of macropore flow (see also Pirastru, Marrosu, et al., 2017, for details). The large-block K_s values were in the same order of magnitude of the $K_{s,I}$ estimated in this work through the drain measurements. In line with the suggestion of Pachepsky and Hill (2017), the results of the present and previous study by Di Prima et al. (2018) conducted in the same site, highlight the importance of accounting for the combined effects of soil heterogeneity, macropore

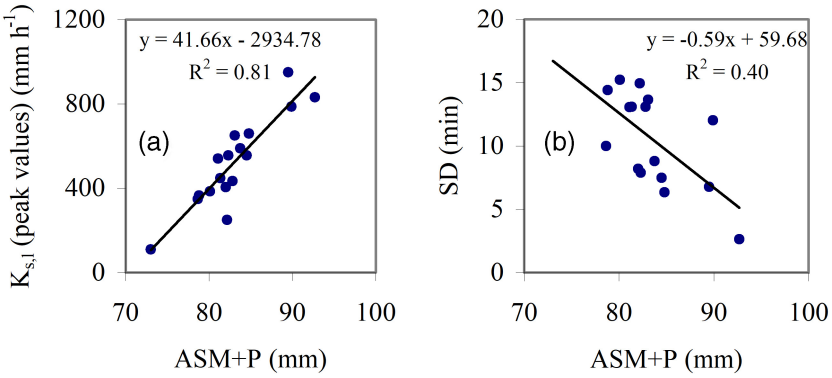

FIGURE 11 Correlations between (a) $K_{s,l}$ values determined at the drainage peaks and ASM + P; (b) standard deviations (SD) of the lag times and ASM + P

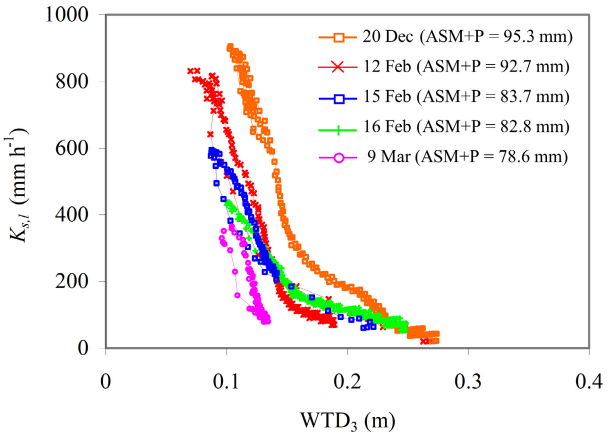

FIGURE 12 Relationships between $K_{s,l}$, and WTD_3 for five drainage events of 2016 characterized by increasing ASM + P index

network connectivity and anisotropy in the investigations of the saturated hydraulic conductivity. Sidle et al. (2001) demonstrated that macropores in wet soil tend to organize in a spatially extended and interconnected network. However, individual macropores are discontinuous along the slope, as they are limited in extension (rarely over 0.5 m in length). The formation of the complex three-dimensional linkage of macropores across a hillslope is facilitated by a series of discrete zones of high permeability, the so-called nodes of connectivity (Sidle et al., 2001). In our hillslope, decomposed rests of roots or trunks and pockets of organic material in the mineral soil could act as connectivity nodes. These were probably buried by the ploughing following the deforestation of the maquis but are still commonly recoverable at present.

A positive and statistically significant correlation was detected between $K_{s,l}$ determined at the peak drainage and ASM + P. This further supported the link between the lateral hydraulic conductivity and the degree of subsurface hydrological connectivity controlling the drainage intensity during storms.

Comparing sets of events with low and intermediate SD values (Table 3) indicated that the water table peak observed locally in the wells was a weak indicator for the $K_{s,l}$ value reached the peak drainage event. Accordingly, Figure 12 shows different $K_{s,l}$ versus WTD_3 patterns for selected drainage events. Each one shows at the peak similar WTD_3 values but very different $K_{s,l}$ values. The results suggested that the $K_{s,l}$ values were influenced mainly by the effective subsurface hydrological connectivity of flow paths (evaluated by SD in Table 3 and by ASM + P in Figure 12) rather than the local water table depth. This information contrasts with the commonly found functional relationships between soil hydraulic conductivity and soil depth (Ambroise et al., 1996; Brooks et al., 2004). In our case, exponential $K_{s,l}$ (WTD_3) fitting functions also were found (Figure 7b). Because these relationships represent an average of the $K_{s,l}$ values obtained for several drainage events, the proposed relationships could be considered representative of an "intermediate" condition of connectivity of the subsurface flow paths in the hillslope. However, at the scale of single drainage events, $K_{s,l}$ (WTD_3) patterns can differ from the intermediate one, depending on the current degree of hydrological connectivity at the hillslope scale controlled by the ASM + P value.

4.3 | Large scale hydrological connectivity explains the $K_{s,l}$ differences between the short and long drains

The runoff coefficients computed for the 2014–15 period were often greater than one (Figure 3), with maximum values of about two. This indicated that the considered rectangular contributing area (137 m^2) upslope of the 2.5 m long drain underestimated the effective contributing one. An extent of at least double should be accounted for, representing about 60% of the area upslope of the 8.5 long drain (467 m^2). The mean drainage volumes for the event increased after the long drain installation (Table 1). However, the increase in the volumes was not proportional to the drain length increase. This further supported the idea that there was only a moderate increase in the contributing area (only 40%, based on the previous analysis of runoff coefficients) despite the tripling of the drain extent. The slightly concave surface morphology in the upper part of the hillslope may have determined subsurface flow convergence from the sides of the grassland towards the central line of the grassed hillslope (approximately the dashed line in Figure 1a), till to be intercepted by the short drain. It is also probable that along the side of the grassed hillslope, a part of subsurface flow may have been lost towards the adjacent soil covered by Mediterranean maquis rather than feeding the lateral segments of the long drain. Plurennial observation (Pirastru et al., 2014; Pirastru,

Bagarello, et al., 2017) showed that, differently from the grassed soil, the maquis soil rarely was saturated by the rainfall. Moreover, topographic features of the impeding layer, which may differ from those of the soil surface, may have also caused flow convergence. Freer et al. (2002), among the others, showed that the local topography of the bedrock has a crucial role in determining the spatial variation of subsurface flow paths. Hence, the analysis of runoff coefficients and the drained volumes suggests that the S1 segment of the long drain (that is, the short drain, Figure 1b) drained the greatest part of the subsurface volumes, while the S2 and S3 drain segments added in 2016 gave a minor contribution. The outflow rates measured in 2016–2017 did not change significantly compared to the previous two-year period. This can be deduced by visually inspecting the hydrograph peaks shown in Figure 2 or by considering the mean and maximum drainage rates reported in Table 1. This also suggested that, within the 8.5 m long drain, the S1 segment captured the flashy response of the hillslope providing the peaks of the groundwater drainage. The added S2 and S3 segments mainly provided additional slow flow during the recessions limbs of the drainage hydrograph. Different drainage responses between segments of the same drain or trench have been widely documented in the literature. For example, Dusek and Vogel (2016) monitored an 8 m long trench composed of two sections and reported significant variability between the yielded individual subsurface outflows. Anderson et al. (2009) measured outflows from three subsections of a road cut section face. They found that the outflow rate of the central section increased dramatically during some large storms compared to the lateral sections. Bachmair and Weiler (2014) monitored subsurface flow by three trenches consisting of two sections. The trench flow differed significantly between the left and right sections, particularly at the grassland and the coniferous forest sites.

The difference in hydrological response between the central and lateral segments of the long drain could be explained by the difference in the extent of their contributing areas and the spatial scale effects of the hydrological connectivity, which had a primary control on the hillslope response, as described in the previous sections. In fact, in the sizeable contributing area upslope of the S1 segment (plausibly about 60% of the contributing area of the long drain), there was a greater possibility of activating interconnections between isolated patches in the macropore network. Once the large-scale macropore network flow was triggered, it enhanced the hillslope drainage, generating an intense lateral subsurface flow response, such as that observed for the short drain. In the smaller contributing areas of the S2 and S3 drain segments, the triggering effect of the large-scale macropore flow could not become fully effective, so generating only an additional slow response, probably governed by the soil matrix. The supposed proportionality between subsurface discharge, mainly driven by macropores, and saturated upslope area, was documented in a hillslope study by Uchida et al. (2004). Moreover, a trench study by Buttle and Turcotte (1999) showed runoff depths and runoff coefficients strongly associated with the extent and, in particular, the volume of the upslope saturated soil layer. Buttle and McDonald (2002) highlighted the importance of the event and pre-event saturated area extension in controlling vertical and lateral flow interactions in macropores in the same experimental site.

On an average, the $K_{s,l}$ values of the short drain were higher than those obtained from the long drain at all the WTD_3 values (Figure 7b). This indicated that the S2 and S3 segments added new contributing areas characterized by relatively low hydraulic conductivity. As previously described, in the small contributing areas of the S2 and S3 segments, the macropore drainage was not efficient, so low $K_{s,l}$ values, probably close to those of the soil matrix, could be derived from these parts of the long drain. As consequence, we expect that the $K_{s,l}$ values shown in Figure 7 for the long drain result from an average of the high values deriving from the S1 segment (or short drain) with the lower ones expected for the S2 and S3 segments, thus providing the lateral saturated hydraulic conductivity at the hillslope scale.

The experimental approach used in this research allowed us to investigate fundamental hydrological processes driving the hillslope response and their spatial variability, and obtain information about the $K_{s,l}$ values for the hillslope scale. Compared to the monitoring scheme of Brooks et al. (2004), we eliminated the lateral barriers for confining lateral flow. While some uncertainty in the $K_{s,l}$ estimation has to be accepted (i.e., lateral losses to the flow domain, non-orthogonality of flow lines to the drain line), the simplification is probably necessary to consider the method as a standard approach for the large-scale investigations. Pirastru, Bagarello, et al. (2017) indicated that using the topographic gradient in place of the hydraulic gradient in this hillslope introduced negligible errors in the computed $K_{s,l}$, particularly for the highest $K_{s,l}$ values. This will minimize the extent of the well network, provided that the sole scope of the investigation is the $K_{s,l}$ evaluation. Implementing irrigation experiments, such as those performed by Pirastru, Bagarello, et al. (2017), could be convenient for estimating $K_{s,l}$ within a few days of experimental campaign. In the future, we aim to perform similar drainage experiments in other hillslopes, forced by artificial rainfall to evaluate the minimum spatial extent of investigation necessary to obtain representative values of $K_{s,l}$ at the hillslope scale.

5 | CONCLUSION

The present study investigated the link between lateral subsurface flow, lateral saturated soil hydraulic conductivity, and hydrological connectivity in a steep hillslope of a Mediterranean basin. Two drains intercepted the subsurface flow with different lengths, that is, short and long drains. The water table level and the soil moisture in a measurement network upslope of the drains were monitored for 4 years.

For both short and long drains, the experimental relationships between the drainage rates and the water table levels were highly non-linear, with a sharp increase of discharge for water table heights close to the soil surface. The research results showed that such an increase could be attributed to an exponential increase of the $K_{s,l}$ in the root zone, reaching values in the order of magnitude of thousands of mm h^{-1} close to the soil surface. Such high values suggested the

presence of active flow in the macropores in the root zone, governing the lateral water transfer for the largest saturated soil thicknesses.

The analysis of the lag times of the water table responses with respect to the drainage peaks indicated the importance of the timing of water table rise in determining the magnitude of drainage response. Observed short lag times and synchronicity of the peaks (evaluated by the standard deviation of the lag times) indicated coupling of the local water table rise with the large-scale subsurface flow generation process, which was fundamental to triggering intense drainage responses. As a driving process, we suggested that the hydrological connectivity of the lateral flow paths throughout the hillslope determined the magnitude of the subsurface hydrological response. Macropores play a primary role in realizing interconnected flow paths, and in favourable hydrological conditions, they could organize in a large-scale network. We also suggest that the spatial extent of the network of interconnected flow paths determined the magnitude of the subsurface flow. By tripling the length of the drain, we obtained only a moderated gain of the contributing area and of the extent of the network of interconnected macropores potentially feasible in wet conditions. This could explain the weaker response (for a unit of length of drain) of the long drain than the short one. The temporal variability of Δt_L and SD between events indicated that the hydrological connectivity of the subsurface flow paths was a dynamic property, depending on the transient hydrologic conditions of the soil. The indicator ASM + P was found to be significantly correlated with Δt_L and SD. Thus it could be conveniently used to evaluate the hydrological connectivity status and better predict the hydrological response of the hillslope.

Provided that the hydrological connectivity of flow paths has a crucial role in determining the hydrological response of the hillslope, it should be adequately considered and parameterized in hydrological modelling. This study suggests that $K_{s,l}$, which is already parameterized in many hydrological models, should be evaluated at the hillslope scale to embed information on hydrological connectivity. However, in natural hillslopes, the quantification of the $K_{s,l}$ depends on the choice of the cross-sectional flow areas and hydraulic gradients in Darcy law, which are subjected to uncertainty due to spatial variability of the saturated soil thickness above the impeding layer. Moreover, macropore flow, particularly the pipe flow, possibly occurring in the large pore networks of the hillslope, likely violates the assumption of laminar flow. Future efforts will be directed to validate the obtained $K_{s,l}$-WTD_3 relationships by modelling the hydrological processes at the hillslope scale.

AUTHOR CONTRIBUTIONS

Mario Pirastru and Massimo Iovino developed the hydrological analysis. Roberto Marrosu, Simone Di Prima, Filippo Giadrossich, and Hassan Awada acquired and provided the field data. Mario Pirastru coordinated the team and supervised the research. All the authors analysed the results and contributed to writing and revising the manuscript.

ACKNOWLEDGEMENTS

This paper is dedicated to the memory of our friend and colleague, Prof. Marcello Niedda. The authors wish to thank Prof. Vincenzo Bagarello for the helpful suggestions. This research was funded by the *HYDROSARD* project of Regione Autonoma Sardegna and FAR2019-PIRASTRU and FAR2020PIRASTRUMA funds of Sassari University. Open Access Funding provided by Universita degli Studi di Sassari within the CRUI-CARE Agreement.

DATA AVAILABILITY STATEMENT

The data that support the findings of this study are available from the corresponding author upon reasonable request.

ORCID

Mario Pirastru https://orcid.org/0000-0001-6641-7026
Massimo Iovino https://orcid.org/0000-0002-3454-2030
Simone Di Prima https://orcid.org/0000-0002-5066-3430
Filippo Giadrossich https://orcid.org/0000-0002-7546-1632
Hassan Awada https://orcid.org/0000-0002-4022-2746

REFERENCES

Ambroise, B., Beven, K., & Freer, J. (1996). Toward a generalization of the TOPMODEL concepts: Topographic indices of hydrological similarity. *Water Resources Research*, *32*(7), 2135–2145. https://doi.org/10.1029/95WR03716

Anderson, A. E., Weiler, M., Alila, Y., & Hudson, R. O. (2009). Subsurface flow velocities in a hillslope with lateral preferential flow. *Water Resources Research*, *45*(11). https://doi.org/10.1029/2008WR007121

Bachmair, S., Weiler, M., & Troch, P. A. (2012). Intercomparing hillslope hydrological dynamics: Spatio-temporal variability and vegetation cover effects. *Water Resources Research*, *48*(5). https://doi.org/10.1029/2011WR011196

Bachmair, S., & Weiler, M. (2014). Interactions and connectivity between runoff generation processes of different spatial scales. *Hydrological Processes*, *28*(4), 1916–1930. https://doi.org/10.1002/hyp.9705

Blain, C. A., & Milly, P. C. D. (1991). Development and application of a hillslope hydrologic model. *Advances in Water Resources*, *14*(4), 168–174. https://doi.org/10.1016/0309-1708(91)90012-D

Brooks, E. S., Boll, J., & McDaniel, P. A. (2004). A hillslope-scale experiment to measure lateral saturated hydraulic conductivity. *Water Resources Research*, *40*(4), W04208. https://doi.org/10.1029/2003WR002858

Brooks, E. S., Boll, J., & McDaniel, P. A. (2007). Distributed and integrated response of a geographic information system-based hydrologic model in the eastern Palouse region, Idaho. *Hydrological Processes*, *21*(1), 110–122. https://doi.org/10.1002/hyp.6230

Buttle, J. M., & McDonald, D. J. (2002). Coupled vertical and lateral preferential flow on a forested slope. *Water Resources Research*, *38*((5)), 18-1–18-16. https://doi.org/10.1029/2001WR000773

Buttle, J. M., & Turcotte, D. S. (1999). Runoff processes on a forested slope on the Canadian shield. *Hydrology Research*, *30*(1), 1–20. https://doi.org/10.2166/nh.1999.0001

Chappell, N. A., Franks, S. W., & Larenus, J. (1998). Multi-scale permeability estimation for a tropical catchment. *Hydrological Processes*, *12*(9), 1507–1523. https://doi.org/10.1002/(SICI)1099-1085(199807)12:9<1507::AID-HYP653>3.0.CO;2-J

Chappell, N. A., & Lancaster, J. W. (2007). Comparison of methodological uncertainties within permeability measurements. *Hydrological Processes*, *21*(18), 2504–2514. https://doi.org/10.1002/hyp.6416

Childs, E. C. (1971). Drainage of groundwater resting on a sloping bed. *Water Resources Research*, *7*(5), 1256–1263. https://doi.org/10.1029/WR007i005p01256

Di Prima, S., Marrosu, R., Lassabatere, L., Angulo-Jaramillo, R., & Pirastru, M. (2018). In situ characterization of preferential flow by combining plot- and point-scale infiltration experiments on a hillslope.

Journal of Hydrology, *563*, 633–642. https://doi.org/10.1016/j.jhydrol.2018.06.033

Dusek, J., & Vogel, T. (2016). Hillslope-storage and rainfall-amount thresholds as controls of preferential stormflow. *Journal of Hydrology*, *534*, 590–605. https://doi.org/10.1016/j.jhydrol.2016.01.047

Freer, J., McDonnell, J. J., Beven, K. J., Peters, N. E., Burns, D. A., Hooper, R. P., Aulenbach, B. T., & Kendall, C. (2002). The role of bedrock topography on subsurface storm flow. *Water Resources Research*, *38*((12)), 5-1–5-16. https://doi.org/10.1029/2001WR000872

Haught, D. R. W., & Meerveld, H. J. (2011). Spatial variation in transient water table responses: Differences between an upper and lower hillslope zone. *Hydrological Processes*, *25*(25), 3866–3877. https://doi.org/10.1002/hyp.8354

Hopp, L., & McDonnell, J. J. (2009). Connectivity at the hillslope scale: Identifying interactions between storm size, bedrock permeability, slope angle and soil depth. *Journal of Hydrology*, *376*(3–4), 378–391. https://doi.org/10.1016/j.jhydrol.2009.07.047

Kim, J., & Mohanty, B. P. (2016). Influence of lateral subsurface flow and connectivity on soil water storage in land surface modeling: Lateral subsurface flow and connectivity. *Journal of Geophysical Research: Atmospheres*, *121*(2), 704–721. https://doi.org/10.1002/2015JD024067

Matonse, A. H., & Kroll, C. N. (2013). Applying hillslope-storage models to improve low flow estimates with limited streamflow data at a watershed scale. *Journal of Hydrology*, *494*, 20–31. https://doi.org/10.1016/j.jhydrol.2013.04.032

McDaniel, P. A., Regan, M. P., Brooks, E., Boll, J., Barndt, S., Falen, A., Young, S. K., & Hammel, J. E. (2008). Linking fragipans, perched water tables, and catchment-scale hydrological processes. *Catena*, *73*(2), 166–173. https://doi.org/10.1016/j.catena.2007.05.011

Michaelides, K., & Chappell, A. (2009). Connectivity as a concept for characterizing hydrological behaviour. *Hydrological Processes*, *23*(3), 517–522. https://doi.org/10.1002/hyp.7214

Montgomery, D. R., & Dietrich, W. E. (1995). Hydrologic processes in a low-gradient source area. *Water Resources Research*, *31*(1), 1–10. https://doi.org/10.1029/94WR02270

Niedda, M. (2004). Upscaling hydraulic conductivity by means of entropy of terrain curvature representation. *Water Resources Research*, *40*(4). https://doi.org/10.1029/2003WR002721

Niedda, M., & Pirastru, M. (2013). Hydrological processes of a closed catchment-lake system in a semi-arid Mediterranean environment. *Hydrological Processes*, *27*(25), 3617–3626. https://doi.org/10.1002/hyp.9478

Niedda, M., & Pirastru, M. (2014). Field investigation and modelling of coupled stream discharge and shallow water-table dynamics in a small Mediterranean catchment (Sardinia). *Hydrological Processes*, *28*(21), 5423–5435. https://doi.org/10.1002/hyp.10016

Niedda, M., Pirastru, M., Castellini, M., & Giadrossich, F. (2014). Simulating the hydrological response of a closed catchment-lake system to recent climate and land-use changes in semi-arid Mediterranean environment. *Journal of Hydrology*, *517*, 732–745. https://doi.org/10.1016/j.jhydrol.2014.06.008

Ocampo, C. J., Sivapalan, M., & Oldham, C. (2006). Hydrological connectivity of upland-riparian zones in agricultural catchments: Implications for runoff generation and nitrate transport. *Journal of Hydrology*, *331*(3–4), 643–658. https://doi.org/10.1016/j.jhydrol.2006.06.010

Pachepsky, Y., & Hill, R. L. (2017). Scale and scaling in soils. *Geoderma*, *287*, 4–30. https://doi.org/10.1016/j.geoderma.2016.08.017

Penna, D., Mantese, N., Hopp, L., Dalla Fontana, G., & Borga, M. (2015). Spatio-temporal variability of piezometric response on two steep alpine hillslopes. *Hydrological Processes*, *29*(2), 198–211. https://doi.org/10.1002/hyp.10140

Pirastru, M., Bagarello, V., Iovino, M., Marrosu, R., Castellini, M., Giadrossich, F., & Niedda, M. (2017). Subsurface flow and large-scale lateral saturated soil hydraulic conductivity in a Mediterranean hillslope with contrasting land uses. *Journal of Hydrology and Hydromechanics*, *65*(3), 297–306. https://doi.org/10.1515/johh-2017-0006

Pirastru, M., Marrosu, R., Di Prima, S., Keesstra, S., Giadrossich, F., & Niedda, M. (2017). Lateral saturated hydraulic conductivity of soil horizons evaluated in large-volume soil monoliths. *Water*, *9*(11), 862. https://doi.org/10.3390/w9110862

Pirastru, M., Niedda, M., & Castellini, M. (2014). Effects of maquis clearing on the properties of the soil and on the near-surface hydrological processes in a semi-arid Mediterranean environment. *Journal of Agricultural Engineering*, *45*(4), 176. https://doi.org/10.4081/jae.2014.428

Scherrer, S., Naef, F., Faeh, A. O., & Cordery, I. (2007). Formation of runoff at the hillslope scale during intense precipitation. *Hydrology and Earth System Sciences*, *11*(2), 907–922. https://doi.org/10.5194/hess-11-907-2007

Sidle, R. C., Noguchi, S., Tsuboyama, Y., & Laursen, K. (2001). A conceptual model of preferential flow systems in forested hillslopes: Evidence of self-organization. *Hydrological Processes*, *15*(10), 1675–1692. https://doi.org/10.1002/hyp.233

Sidle, R. C., Tsuboyama, Y., Noguchi, S., Hosoda, I., Fujieda, M., & Shimizu, T. (2000). Stormflow generation in steep forested headwaters: A linked hydrogeomorphic paradigm. *Hydrological Processes*, *14*(3), 369–385. https://doi.org/10.1002/(SICI)1099-1085(20000228)14:3<369::AID-HYP943>3.0.CO;2-P

Smith, M. W., Bracken, L. J., & Cox, N. J. (2010). Toward a dynamic representation of hydrological connectivity at the hillslope scale in semiarid areas. *Water Resources Research*, *46*(12). https://doi.org/10.1029/2009WR008496

Stieglitz, M., Shaman, J., McNamara, J., Engel, V., Shanley, J., & Kling, G. W. (2003). An approach to understanding hydrologic connectivity on the hillslope and the implications for nutrient transport. *Global Biogeochemical Cycles*, *17*((4)). https://doi.org/10.1029/2003GB002041

Troch, P. A., Paniconi, C., & Emiel van Loon, E. (2003). Hillslope-storage Boussinesq model for subsurface flow and variable source areas along complex hillslopes: 1 Formulation and characteristic response. *Water Resources Research*, *39*(11). https://doi.org/10.1029/2002WR001728

Tromp-van Meerveld, H. J., & McDonnell, J. J. (2006). On the interrelations between topography, soil depth, soil moisture, transpiration rates and species distribution at the hillslope scale. *Advances in Water Resources*, *29*(2), 293–310. https://doi.org/10.1016/j.advwatres.2005.02.016

Uchida, T., Asano, Y., Mizuyama, T., & McDonnell, J. J. (2004). Role of upslope soil pore pressure on lateral subsurface storm flow dynamics. *Water Resources Research*, *40*(12). https://doi.org/10.1029/2003WR002139

Uchida, T., Kosugi, K., & Mizuyama, T. (2001). Effects of pipeflow on hydrological process and its relation to landslide: A review of pipeflow studies in forested headwater catchments. *Hydrological Processes*, *15*(11), 2151–2174. https://doi.org/10.1002/hyp.281

van Schaik, N. L. M. B., Schnabel, S., & Jetten, V. G. (2008). The influence of preferential flow on hillslope hydrology in a semi-arid watershed (in the Spanish Dehesas). *Hydrological Processes*, *22*(18), 3844–3855. https://doi.org/10.1002/hyp.6998

Weiler, M., McDonnell, J. J., Tromp-van Meerveld, I., & Uchida, T. (2006). Subsurface stormflow. In M. G. Anderson & J. J. McDonnell (Eds.), *Encyclopedia of hydrological sciences*. John Wiley & Sons, Ltd.. https://doi.org/10.1002/0470848944.hsa119

Wienhöfer, J., & Zehe, E. (2014). Predicting subsurface stormflow response of a forested hillslope – The role of connected flow paths. *Hydrology and Earth System Sciences*, *18*(1), 121–138. https://doi.org/10.5194/hess-18-121-2014

How to cite this article: Pirastru, M., Iovino, M., Marrosu, R., Di Prima, S., Giadrossich, F., & Awada, H. (2022). Large-scale lateral saturated soil hydraulic conductivity as a metric for the connectivity of subsurface flow paths at hillslope scale. *Hydrological Processes*, *36*(8), e14649. https://doi.org/10.1002/hyp.14649